

100-Year Lower Mississippi Floods in a Global Climate Model: Characteristics and Future Changes

KARIN VAN DER WIEL,^a SARAH B. KAPNICK,^b GABRIEL A. VECCHI,^{c,d}
JAMES A. SMITH,^e P. C. D. MILLY,^f AND LIWEI JIA^g

^a *Royal Netherlands Meteorological Institute, De Bilt, Netherlands*

^b *NOAA/Geophysical Fluid Dynamics Laboratory, Princeton, New Jersey*

^c *Department of Geosciences, Princeton University, Princeton, New Jersey*

^d *Princeton Environmental Institute, Princeton, New Jersey*

^e *Department of Civil and Environmental Engineering, Princeton University, Princeton, New Jersey*

^f *U.S. Geological Survey, Princeton, New Jersey*

^g *NOAA/NWS/NCEP/Climate Prediction Center, College Park, and Innovim LLC, Greenbelt, Maryland*

(Manuscript received 31 January 2018, in final form 21 May 2018)

ABSTRACT


Floods in the Mississippi basin can have large negative societal, natural, and economic impacts. Understanding the drivers of floods, now and in the future, is relevant for risk management and infrastructure-planning purposes. We investigate the drivers of 100-yr-return lower Mississippi River floods using a global coupled climate model with an integrated surface water module. The model provides 3400 years of physically consistent data from a static climate, in contrast to available observational data (relatively short records, incomplete land surface data, transient climate). In the months preceding the model's 100-yr floods, as indicated by extreme monthly discharge, above-average rain and snowfall lead to moist subsurface conditions and the buildup of snowpack, making the river system prone to these major flooding events. The meltwater from snowpack in the northern Missouri and upper Mississippi catchments primes the river system, sensitizing it to subsequent above-average precipitation in the Ohio and Tennessee catchments. An ensemble of transient forcing experiments is used to investigate the impacts of past and projected anthropogenic climate change on extreme floods. There is no statistically significant projected trend in the occurrence of 100-yr floods in the model ensemble, despite significant increases in extreme precipitation, significant decreases in extreme snowmelt, and significant decreases in less extreme floods. The results emphasize the importance of considering the fully coupled land-atmosphere system for extreme floods. This initial analysis provides avenues for further investigation, including comparison to characteristics of less extreme floods, the sensitivity to model configuration, the role of human water management, and implications for future flood-risk management.

1. Introduction

The Mississippi–Missouri River system (hereafter referred to as the Mississippi River) is one of the largest river systems in the world. Its basin area covers 41% of the contiguous United States and parts of 31 U.S. states (Fig. 1a; Changnon 1998; Wallenfeldt et al. 2015). Economically, the region is of U.S. national importance because, among other reasons, the majority of U.S. agricultural production originates there (Foley et al. 2004).

Furthermore, many flood-vulnerable areas in the catchment are occupied by people and property (Galloway 1995). Anomalous Mississippi River runoff also influences hypoxia conditions in the Gulf of Mexico, impacting U.S. fisheries (Rabalais et al. 1998; Donner and Scavia 2007). For these reasons, flood events pose a risk for U.S. society and create a need for comprehensive studies that investigate the characteristics of such events, now and in the future.

The basin's main vulnerability to flooding arises from the risk of river flooding, which occurs when the amount of surface runoff from a catchment into a river or stream exceeds the channel capacity. In such cases, the water overflows river banks and floods lower-lying land areas. Many factors determine when and where river flooding

 Denotes content that is immediately available upon publication as open access.

Corresponding author: Karin van der Wiel, wiel@knmi.nl

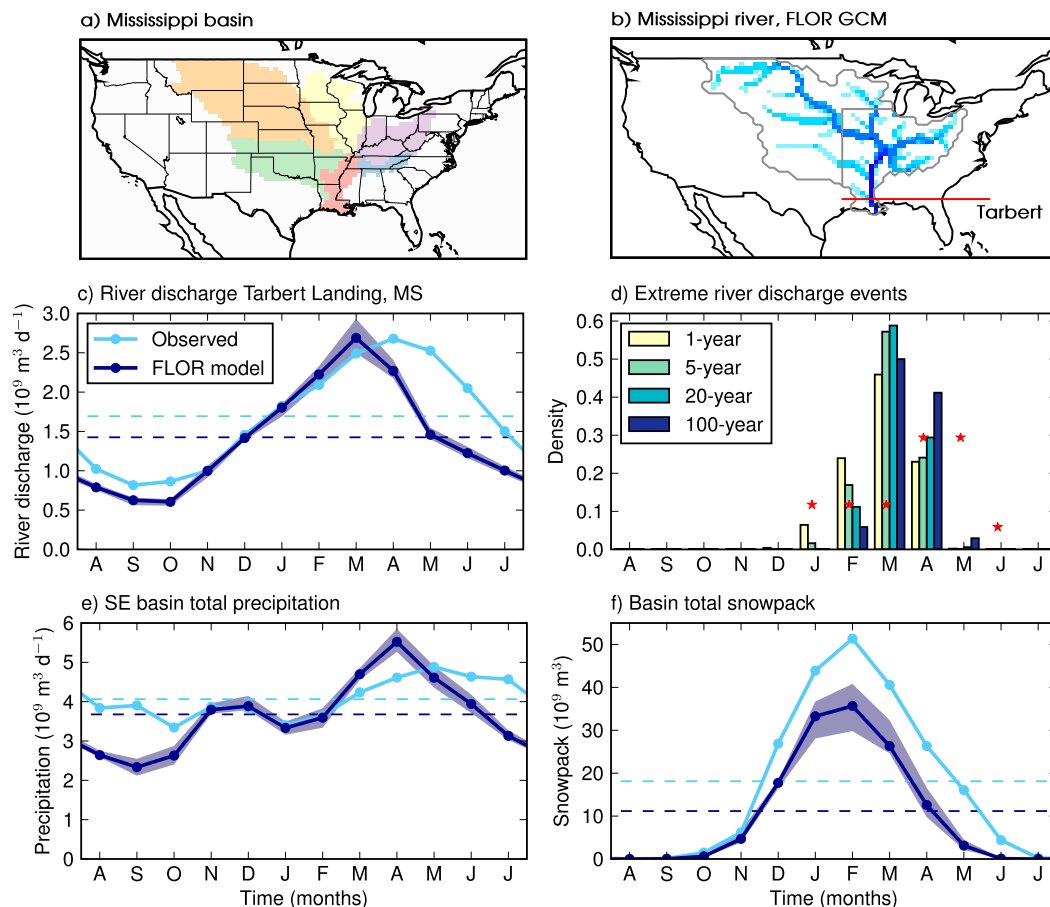


FIG. 1. (a) Mississippi River basin, colored by hydrological units: Missouri, upper Mississippi, Ohio (northern units, from west to east), Arkansas–White–Red, lower Mississippi, Tennessee (southern units, from west to east). (b) Mississippi River as simulated in the FLOR GCM; darker blue colors show larger discharges and the red line indicates the latitude of the gauge at Tarbert Landing, MS, in the real world. (c) Annual cycle of river discharge at Tarbert Landing as observed (light blue) and as simulated in the FLOR GCM (dark blue; shading shows range of individual ensemble members). Dashed lines show the annual mean value. (d) Annual distribution of simulated extreme river discharge events, for 1-, 5-, 20-, and 100-yr return events. Red stars indicate values for the 5-yr return event in observed river discharge. (e) As in (c), but for southeast basin total precipitation. (f) As in (c), but for basin total snowpack.

occurs: basin characteristics (e.g., size, topography, soil type), preexisting land conditions (e.g., soil moisture content, total water in the river system, snowpack), fluxes of water (e.g., rainfall, snowfall, evaporation, snowmelt), human decision-making (e.g., land use, river management, engineering structures), and interactions among all of those factors (e.g., Kunkel et al. 1999; De Michele and Salvadori 2002; Merz and Blöschl 2003; Pinter et al. 2006; Trambly et al. 2010). River systems connect large areas of land, so local flooding may be the result of conditions upstream or downstream.

The Mississippi River has historically experienced large floods, produced by a variety of natural causes. The largest floods in the last century occurred in 1927, 1937, 1973, and 2011; these resulted principally from heavy

rainfall in the lower Mississippi and Ohio River basins (Lott and Myers 1956; Myers 1959; Smith and Baeck 2015). Previous research has linked anomalously large water vapor transport from the Gulf of Mexico to the continental United States at monthly time scales to extreme flooding events (Smith and Baeck 2015; Benedict et al. 2018). Furthermore, land conditions may prime the river system and make a catchment more susceptible to flooding; for example, frozen soil limits the infiltration capacity of the soil leading to a larger fraction of snowmelt or precipitation becoming surface runoff, potentially causing flooding (Cherkauer and Lettenmaier 1999; Bayard et al. 2005). Floods in the northern Mississippi basin are mostly snowmelt dominated (Camillo 2012; Olsen et al. 1999).

Understanding the characteristics, magnitude, and frequency of floods is vital for flood-risk management. Such information is used when planning land use in flood plains, both for agriculture and buildings. Infrastructure projects, for example, bridges or dams, are built under specific assumptions of river flooding statistics (Hodgkins et al. 2017). Extreme flooding events with long return times are of special interest, as flood defenses and other manmade structures are often designed to withstand such events. The 100-yr event that is primarily studied here is a representative choice: it has a 1% annual chance of occurring. It is of societal relevance as it has been chosen by the U.S. Federal Emergency Management Agency (FEMA) to define flood-hazard areas and to communicate flood risk to U.S. citizens (FEMA 2017).

Under climate change, flood-risk management is a moving target, given changes in meteorological and land conditions that lead to flood events. Future conditions have to be taken into account when planning new buildings or infrastructure projects. It is not clear a priori whether flood risk will increase, decrease, or remain constant. Flood maps therefore have to be regularly updated to reflect changing probabilities. For observed mean Mississippi discharge, increasing trends are reported (Zhang and Schilling 2006; USGCRP 2017). However, the river exhibits decadal variability related to El Niño–Southern Oscillation and the Atlantic multi-decadal oscillation, which complicates trend analysis on relatively short records (Munoz et al. 2018), and evolving human river management masks flood risk changes due to natural causes or climate change (Zhang and Schilling 2006; Munoz et al. 2018; George 2018). Modeling studies show varying trends in river discharge for basins globally; for the Mississippi River, most report a slight decrease of mean flow and flood risk (e.g., Nijssen et al. 2001; Milly et al. 2002; Arnell 2003; Aerts et al. 2006; Zhang and Schilling 2006; Hirabayashi et al. 2013; Van Vliet et al. 2013).

To explore the atmospheric and land surface drivers of extreme lower Mississippi River flood events, we use a fully coupled global climate model (GCM) in the current study. A model approach is useful to complement empirical studies because observational data series do not cover sufficiently long periods to investigate the multitude of causes of the most extreme floods. Crucially, the land component of the GCM used here includes a surface water (river and lake) module. Interactions between land, atmosphere, ocean, and cryosphere are therefore explicitly modeled, including their effects on river discharge amounts. The novel GCM approach in the current study allows us to select events by a variable very closely related to societal impacts—extreme high river discharge—and investigate the associated forcing from

land and atmosphere in a physically consistent, global system. This approach is fundamentally different from a purely meteorological approach (i.e., the investigation of the rain events that have been previously linked to flood conditions), and also differs from a sequential model approach (i.e., forcing a hydrological model with climate data). Our impact-based approach guarantees the highest discharge events are investigated, independent of the processes that cause them, and allows for an analysis of the interaction among all variables influencing extreme river discharge.

The GCM provides a complete water budget closure, allowing for long experimental integrations and understanding of how seasons in advance of a flood event may contribute to flood risk. In regional climate models or integrations of land surface models forced by meteorological boundary conditions there is no closure of the water budget, and this can be an issue when land–atmosphere feedbacks or processes on long time scales are studied (Milly and Dunne 2017). A model approach also has disadvantages, most notably that biases in modeled fields may impact findings, and parameterization schemes may misrepresent important processes. Though GCMs undergo constant improvements, the surface water module used here is simpler than state-of-the-art hydrological models. The presented results must therefore be considered with model limitations and biases in modeled fields in mind. We evaluate model biases and discuss their impact and consequences in the paper.

By prescribing time-varying atmospheric concentrations of greenhouse gases, ozone and aerosols (both volcanic and anthropogenic), and solar variations, we investigate the impact of anthropogenic climate change on river floods. The climate change response of snowmelt (likely decreasing, earlier melt; Nijssen et al. 2001; Kapnick and Delworth 2013) and extreme precipitation (likely increasing; O’Gorman 2015; Van der Wiel et al. 2016) may have opposite effects on extreme river discharge. The GCM and impact-based approach used here allows us to investigate the total effect of climate change on Mississippi River flooding.

We select events with extreme high monthly mean river discharge. Note that, though a river basin acts to integrate weather events over space and time into a common discharge variable, instantaneous discharge peaks exceed monthly discharge peaks (Fig. 2). Here, given the significant correlation between daily discharge peaks and monthly mean values ($r = 0.94$), it is assumed that extreme high monthly mean values are a good indicator for flood conditions. However, individual weather events cannot be directly linked to variations in discharge. Our analysis provides information regarding the physical mechanisms that cause discharge

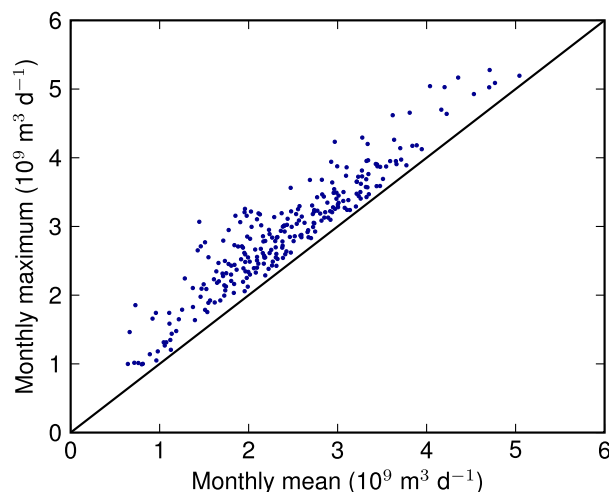


FIG. 2. Scatterplot of monthly mean river discharge and monthly maximum river discharge based on daily values (FMA only). Observed data for Tarbert Landing, 1930–2016.

variability at monthly time scales. This contributes toward understanding the atmospheric and land forcing of extreme Mississippi flooding; further work is needed to investigate the characteristics of discharge variability at shorter time scales.

In this paper we focus on major Mississippi River flood events in the GCM, as defined by extreme high monthly mean river discharge (discharge exceeding the level associated with a mean return period of 100 years) at a location near the river mouth. We investigate three aspects of the problem: 1) the atmospheric and land processes that lead to extreme high discharge events in a preindustrial climate, 2) potential predictability of those extreme high discharge events, and 3) changes in Mississippi extreme high discharge events due to anthropogenic climate change. The remainder of this paper is organized as follows: the coupled GCM and experimental design are described in section 2, followed by a description of the analysis methods and model biases in section 3. The climatic characteristics of Mississippi extreme high discharge events in the model are described in section 4, an assessment of predictability of high discharge events in the model is given in section 5, and potential changes due to global warming are discussed in section 6. Section 7 provides a summary and a final discussion.

2. Model and experiment description

We used the National Oceanic and Atmospheric Administration (NOAA) Geophysical Fluid Dynamics Laboratory (GFDL) Forecast-Oriented Low-Ocean Resolution (FLOR) fully coupled GCM. FLOR is built

from relatively high-resolution atmosphere and land components ($0.5^\circ \times 0.5^\circ$ global grid), coupled to lower-resolution ocean and sea ice components ($1^\circ \times 1^\circ$ global grid). FLOR was built from two widely used GFDL models: the low-resolution CM2.1 (Delworth et al. 2006) and the high-resolution CM2.5 (Delworth et al. 2012). Slight differences exist between the components of FLOR and those in CM2.1/CM2.5, and these are described in more detail in Jia et al. (2015) and Van der Wiel et al. (2016). Here we used the flux-adjusted version of FLOR (Vecchi et al. 2014). Atmosphere-to-ocean fluxes of momentum, enthalpy, and freshwater are artificially adjusted to bring the model-simulated sea surface temperature and the wind stress felt by the ocean closer to observed fields. Once coupled, the flux adjustments are interannually constant and independent of the state of the model climate system. The full adjustment procedure is described in Vecchi et al. (2014).

The land model component of FLOR is a variant of the LM3.0 described by Milly et al. (2014). It includes interactive vegetation cover (as in Shevliakova et al. 2009), snowpack, subsurface freeze–thaw, groundwater, and surface waters. Rainfall and snowmelt either infiltrate or run off, depending on soil wetness and thermal state. That which infiltrates is stored for variable amounts of time until it is released as subsurface runoff to join the surface runoff and enter the surface water system. The surface water module transports the runoff through grid-scale river reaches and lakes to the ocean; the Mississippi River as simulated in FLOR is shown in Fig. 1b. There is generally a time lag between precipitation and downstream discharge. The time lag is a result of multiple stores: snowpack, soil water, groundwater, and lake and river water. A water balance for the system (excluding snowpack) can be expressed as

$$R + S = (P_{\text{NF}} - E) + \text{SM}, \quad (1)$$

in which P_{NF} is nonfrozen precipitation, E is evapotranspiration from soil, SM is snowmelt rate, R is runoff, and S is storage in the subsurface. The presence of S means that runoff is not contemporaneous with P_{NF} or SM.

The study was based on two types of experiments, each with a distinct aim. First, the model was integrated for 3500 years using constant atmospheric composition and land-use conditions as in the year 1860 (the 1860 control experiment). The first 100 years of the control experiment were removed to allow for model spinup. The remaining 3400 years were used to analyze extreme Mississippi high discharge events in a stationary climate. There is no forced variability in this experimental setup, so all variability in the experiment is the result of internal climate variability. It is assumed that slow model

drift, caused by top-of-the-atmosphere radiative disequilibria and slow ocean adjustments, has limited impact on the results. This 1860 control experiment allows for investigation of the characteristics of flooding events in a stationary climate, enabling us to identify mechanisms without the results being clouded by possible changes due to anthropogenic climate change. The experiment was previously used to study other aspects of the climate, for example, U.S. heat waves (Jia et al. 2016), eastern Pacific tropical cyclones (Murakami et al. 2017), and extreme precipitation in the United States and India (Van der Wiel et al. 2017; Krishnamurthy et al. 2018).

Our experiences in the real world, and the full observational record, represent a post-1860 transient climate. Therefore, we use a second transient forcing model experiment in which time-varying atmospheric greenhouse gases, ozone, and aerosol concentrations were prescribed (Jia et al. 2016). The aim of this experiment was to investigate the response of Mississippi high discharge events to historic and future projected atmospheric compositions and to provide a dataset that could be directly compared to the observed record (e.g., Figs. 1c–f). An ensemble of five model integrations from 1861 to 2100 (in total 1200 years of data) was used to find potential changes in return times of the high discharge events and investigate potential changes of river water sources. Years 101, 121, 141, 161, and 181 from the 1860 control experiment were used to provide initial conditions for these integrations. Model years 1861–2005 used historical forcing, and projected forcing in model years 2006–2100 was based on representative concentration pathway 4.5 (RCP4.5; Van Vuuren et al. 2011).

The exceptional length of the model integrations means that the most extreme events are explicitly modeled, and their characteristics can be investigated without having to rely on statistical formulations of the tail of the distribution. It is important to create an adequate sample of major discharge events, as different events may be caused by different mechanisms. Also, it is unlikely that a 100-yr flooding event occurs once every 100 years. In Fig. 3a we show that the estimate of the extreme discharge magnitude indeed converges for longer time series. Though the median estimate is very close to the best estimate for all calculations, the range of possible estimates decreases rapidly for longer integrations. For time series of 500 years in length, the estimate varies between 4.96 and $6.00 \times 10^9 \text{ m}^3 \text{ day}^{-1}$, and for time series of 2000 years in length the range decreases to 5.22 – $5.54 \times 10^9 \text{ m}^3 \text{ day}^{-1}$. The chance of underestimating (potentially leading to a false sense of security) or overestimating (potentially leading to unnecessary adaptation and management expenses)

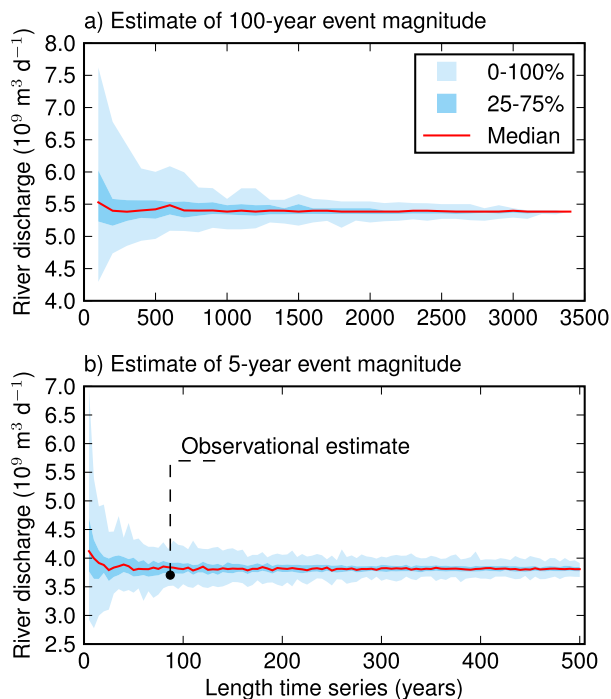


FIG. 3. Estimated magnitude of extreme high discharge events of a chosen return period based on samples of different lengths from the 1860 control experiment. Samples were created by means of bootstrapping X years (x axis) from the full experiment. Blue shading indicates the full range of estimates (lighter) and the interquartile range (darker), and the red line indicates the median estimate. Shown are (a) events of average 100-yr return period and (b) events of average 5-yr return period. The black dot in (b) shows the estimated 5-yr magnitude based on the 87-yr observational record.

extreme high discharge magnitudes decreases when long time series are used.

3. Methods

We analyzed high discharge events near the mouth of the Mississippi River. In the model, we chose the grid cell where the river crosses 31.25°N (red line in Fig. 1b). This is the latitude of the gauge at Tarbert Landing, Mississippi, in the real river. Because the real river bifurcates north of this latitude, for our observational estimate we summed the gauged discharges of the Mississippi River at Tarbert Landing and the Atchafalaya River at Simmesport, Louisiana.¹

Based on time series of monthly river discharge, we defined Mississippi extreme high discharge events as those occurring during months when river discharge exceeded a level associated with a chosen return period.

¹ Data downloaded from <http://rivergages.mvr.usace.army.mil/>, gauge IDs 01100Q and 03045Q, accessed 22 August 2017.

This threshold level is determined for each experiment separately. The major Mississippi flood events that are the focus of this study were defined to have an average return period of 100 years.

To quantify model biases, we first focus on the annual cycles of river discharge, precipitation and snowpack, and the timing of flooding events with a lower return period. The observed record from 1930 to 2016 is not of sufficient length to adequately sample and characterize the typical 100-yr flooding event (Fig. 3) without complex statistical extrapolation methods for defining extremes. With the availability of thousands of years of data from a climate model, we can explore and characterize extreme events from model output directly. Therefore, we compare the seasonal timing of 5-yr events, which can be better sampled from the available observations. Note that model biases for low extreme events are not necessarily comparable to model biases for high extreme events, since the mechanisms for each may be different.

In the natural environment, flood events have been linked to high precipitation amounts in the Ohio, Tennessee, and lower Mississippi catchments (the project design flood, Hypo-Flood 58A; Lott and Myers 1956; Myers 1959; Olsen et al. 1999; Camillo 2012; Smith and Baeck 2015). We therefore investigate GCM biases in precipitation in this region (south of 42.5°N, east of 95.0°W, area gray outlined in Fig. 1b). In the annual mean, the model has a low bias of $0.39 \times 10^9 \text{ m}^3 \text{ day}^{-1}$, though the spring peak is stronger than observed (Fig. 1e).² Furthermore, as stated before, snowmelt has been linked to causing floods in the north of the basin. The GCM captures the seasonal cycle of snowpack well, though the winter peak in February is $16 \times 10^9 \text{ m}^3$ lower than observed (Fig. 1f).³

The precipitation bias, and further model biases (e.g., in evaporation, timing of melt) or missing processes (e.g., irrigation taking water out of the river system), result in biases in Mississippi River discharge. Figure 1c shows the annual cycle of observed combined Mississippi–Atchafalaya River discharge and the corresponding model discharge. The model has a 15% lower annual mean value (1.43 versus $1.69 \times 10^9 \text{ m}^3 \text{ day}^{-1}$) than that observed. The modeled spring discharge maximum is a month early but of approximately the right strength ($0.01 \times 10^9 \text{ m}^3 \text{ day}^{-1}$ difference). The timing bias may be associated with the spring peak of modeled precipitation or the neglect of macropore-assisted

snowmelt infiltration into frozen ground; inclusion of the latter process substantially removes the bias (Milly et al. 2014). Also of possible relevance is the missing influence of anthropogenic water resource management (Harmar et al. 2005; Raymond et al. 2008; Pinter et al. 2010).

Consistent with the early bias in the spring river discharge maximum, 5-yr flooding events in the model occur on average earlier than those in the real world (green bars and red stars in Fig. 1d). Furthermore, the occurrence of 5-yr events in the model is limited to the months of January–May, though most events occur in February–April (FMA). In the observational data, based on a much smaller sample size (17 vs 680 events), these events happened from January to June.

In spite of these model biases, we used the FLOR GCM for the analysis of major Mississippi flooding events. An analysis of such events based on observational data is not possible, given the limited length of reliable river discharge (Fig. 3) and precipitation data. Furthermore, to our best knowledge, long time series with sufficient spatial coverage of snowpack, snowmelt, and other relevant land variables do not exist. As noted in section 1, the use of a GCM with an integrated surface water module allows us to analyze extreme events in a physically consistent framework. In section 7 we will discuss the validity of our model results in the real world.

We analyzed the land and meteorological conditions that give rise to flooding events with an average return period of 100 years. To do so, the 34 most extreme river discharge events to occur in the 1860 control experiment in the months FMA were selected. The selection of events was constrained to a shorter season of flooding to facilitate comparison against other variables that may have different annual cycles and annual maxima. The temporal constraint (months FMA) does not impact the selection of events much: 97% of the modeled annual 100-yr events (33 of 34) and 93% of the annual 1-yr events occur in FMA (Fig. 1d). Composite analysis was performed to analyze the relation of other climatic variables to the selected 34 events.

The response of extreme river discharge to radiative forcing was investigated by means of a peak-over-threshold selection method. Thresholds were determined as before, based on a chosen average return period in the complete transient forcing experiment. The change of probability over time will be noted by means of the risk ratio, the ratio of probabilities from different years (in the current study 2100 versus 1861):

$$\text{risk ratio} = \frac{p_{2100}}{p_{1861}}. \quad (2)$$

A risk ratio close to 1.0 indicates no change in probability ($p_{2100} \approx p_{1861}$), ratios above 1.0 correspond to increased

² Observed data from the NCEP/Climate Prediction Center unified gauge-based analysis of daily precipitation over the contiguous United States, covering 1948–2017 (Higgins et al. 2000).

³ Observed snow water equivalent data from National Operational Hydrologic Remote Sensing Center (2004), covering 2005–17, accessed 20 April 2018.

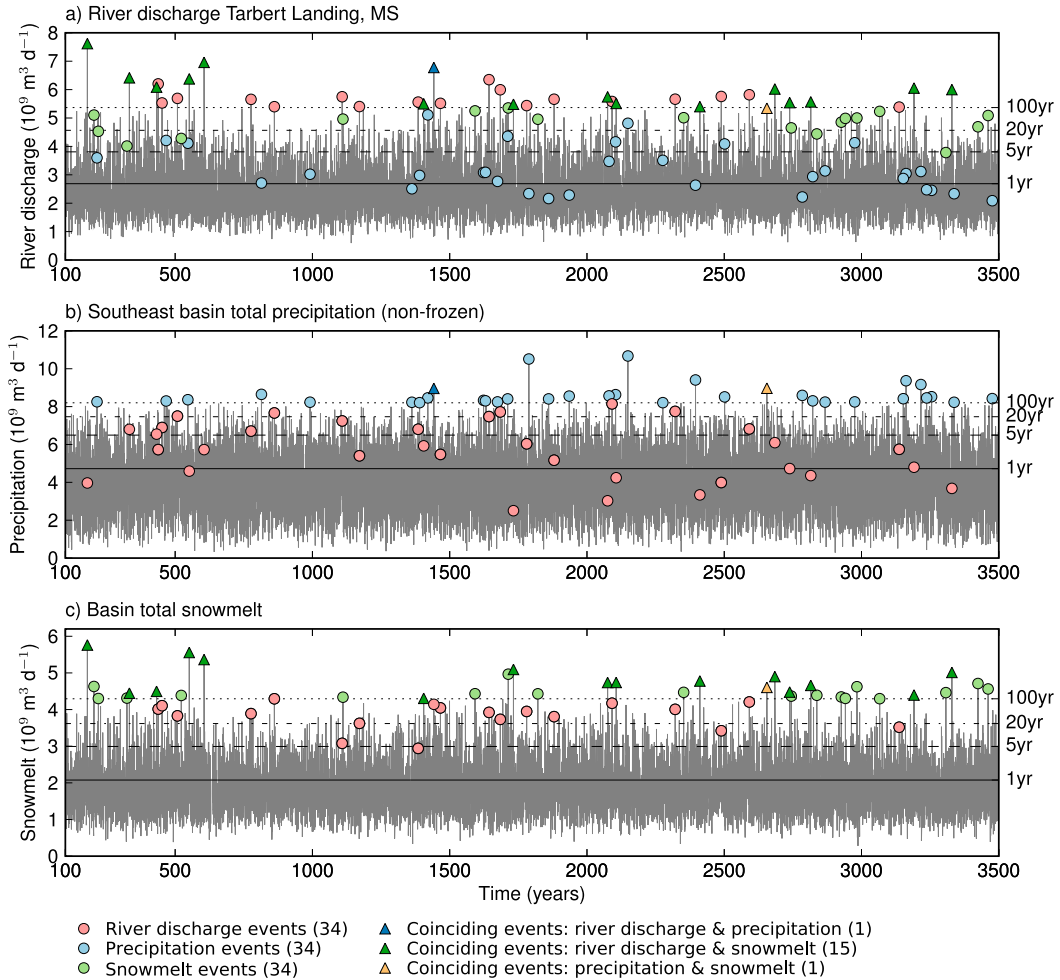


FIG. 4. Time series of monthly mean (a) river discharge at Tarbert Landing, (b) southeast basin total nonfrozen precipitation, and (c) basin total snowmelt, in gray lines. Only the months February–April are shown, i.e., the time series shown is FMAFMA. Colored circles indicate 100-yr return events, selected by river discharge (pink), precipitation (light blue), or snowmelt (light green). Colored triangles indicate coinciding events of discharge and precipitation (dark blue), discharge and snowmelt (dark green), or precipitation and snowmelt (orange). Horizontal solid, dashed, dash-dotted, and dotted lines show the value associated with an event of average 1-, 5-, 20-, and 100-yr return period, respectively.

risk due to climate change ($p_{2100} > p_{1861}$), and ratios below 1.0 correspond to decreased risk ($p_{2100} < p_{1861}$).

4. Characteristics of 100-yr extreme discharge events

Based on 3400 years of simulated river discharge in the 1860 control experiment, the 34 highest discharge events in the months FMA have been selected (pink circles and green/blue triangles in Fig. 4a). The minimum discharge amount associated with these 100-yr events is $5.38 \times 10^9 \text{ m}^3 \text{ day}^{-1}$ (dotted line in Fig. 4a), close to a doubling of the climatological spring discharge maximum ($2.76 \times 10^9 \text{ m}^3 \text{ day}^{-1}$; Fig. 1c).

We investigate the relationship among extreme precipitation events, extreme snowmelt events, and extreme high discharge events by looking at representative time series. For extreme precipitation a southeast basin total time series was computed (as in Fig. 1e). As was done for extreme discharge events, extreme precipitation events with a mean 100-yr return period in FMA in this time series have been selected (blue circles and triangle in Fig. 4b). There is one 100-yr precipitation event that coincides with a 100-yr discharge event (marked by a dark blue triangle); the remaining 33 precipitation events neither coincide with nor immediately precede the largest discharge events. Pink circles in Fig. 4b show the basin total precipitation amounts

associated with the largest discharge events selected from the discharge time series (Fig. 4a). Note that there are extreme discharge events with high precipitation values and extreme discharge events with low precipitation values. Conversely, there are precipitation events with low discharge values and precipitation events with high discharge values (blue circles and triangles in Fig. 4a).

This analysis is repeated for a time series of basin total snowmelt (Fig. 4c). There are 15 coinciding events of extreme snowmelt and river discharge (dark green triangles in Figs. 4a,c). The other snowmelt events do not coincide or immediately precede flooding events (green circles in Figs. 4a,c). There is one coinciding 100-yr event of extreme precipitation and extreme snowmelt (orange triangle in Figs. 4a–c).

The mean river discharge of the selected integrated precipitation events is $3.35 \times 10^9 \text{ m}^3 \text{ day}^{-1}$ (blue circles and triangle in Fig. 4a), the mean river discharge of the selected integrated snowmelt events is $5.35 \times 10^9 \text{ m}^3 \text{ day}^{-1}$ (green circles and triangles in Fig. 4a). Both values are larger than the climatological spring discharge maximum, and the mean discharge of the snowmelt events is close to that associated with 100-yr flood events ($5.38 \times 10^9 \text{ m}^3 \text{ day}^{-1}$).

The above time series analysis was repeated using a time series of total Mississippi River basin precipitation, and the results are qualitatively similar (zero coinciding events precipitation discharge vs 15 coinciding events snowmelt discharge; figure not shown).

Though the main focus of this paper is on major Mississippi flooding events with an average return period of 100 years, here we briefly investigate high discharge events of a smaller return period. The goal of this side step is to investigate whether the relationships between snowmelt and discharge and between precipitation and discharge are comparable for less extreme events, in order to contextualize the calculated flood risks from the short observational record. If less extreme events in the model are fundamentally different from high extreme events in the model, then understanding gained from short records might not be suitable for extrapolation to the most extreme events.

Table 1 shows the number of coinciding events for various combinations of selected extreme events. If one considers less extreme snowmelt or precipitation events (of return period 20 or 5 years) to potentially explain the 100-yr discharge events (top three rows), snowmelt remains the biggest contributor. Note that for snowmelt events smaller than the 5-yr snowmelt, the occurrence of a major river discharge event is almost excluded. If one considers 20-yr events for all three time series, again snowmelt events coincide more frequently with discharge

TABLE 1. Total number of coinciding events in the time series of Fig. 4 and percentage of selected extreme high discharge events in parentheses. Sets of three rows indicate the return period of the river discharge (RD) event considered; columns represent changing return periods for the selected P and SM events. The RD-only values are from Fig. 4.

	P and SM events		
	100-yr	20-yr	5-yr
	RD: 100-yr events (34)		
RD and P	1 (3%)	7 (21%)	14 (41%)
RD and SM	15 (44%)	30 (88%)	33 (97%)
RD and P and SM	0 (0%)	7 (21%)	11 (32%)
	RD: 20-yr events (170)		
RD and P	—	12 (7%)	37 (22%)
RD and SM	—	101 (59%)	153 (90%)
RD and P and SM	—	11 (7%)	31 (18%)
	RD: 5-yr events (680)		
RD and P	—	—	107 (16%)
RD and SM	—	—	412 (61%)
RD and P and SM	—	—	53 (8%)

events (101 of 170 events) than coinciding precipitation and discharge events (12 of 170 events). For all discharge events considered, high snowmelt is a better predictor of high discharge than high precipitation is. Note that, in the model, the relative difference between coinciding discharge–snowmelt events and coinciding discharge–precipitation events is much higher for extreme flooding events (factor of 15 for 100-yr floods) than for less extreme flooding events (factor of 4 for 5-yr floods). This indicates that, in the model, less extreme high discharge events have different characteristics than high extreme high discharge events.

Next, we investigate the spatial patterns of various atmospheric and land variables for the selected extreme discharge events. Figure 5 shows the mean for a number of variables over the selected 34 major flood events. Figure 6 shows the same composites but for anomalies of the variables investigated. By design of the selection method, there is very high discharge in the channel leading to the river mouth (Fig. 5a); anomalous discharge exceeds $3 \times 10^9 \text{ m}^3 \text{ day}^{-1}$ (Fig. 6a). Months of high discharge are characterized by high rain amounts in the southeast of the basin (Figs. 5b, 6b) and snowfall farther north (Figs. 5c, 6c). There is also significant snowmelt in the north of the basin (Figs. 5f, 6f). Evaporation is below normal (Fig. 6d), maybe caused by the below-normal near-surface temperatures (Fig. 6i).

Two fluxes of water (nonfrozen precipitation minus evapotranspiration $P_{\text{NF}} - E$, and SM) combine to lead to some combination of storage of water in the subsurface or on the surface and to runoff (Figs. 5g, 6g), which is input for the modeled river system [Eq. (1)]. During extreme discharge events most river water originates in the

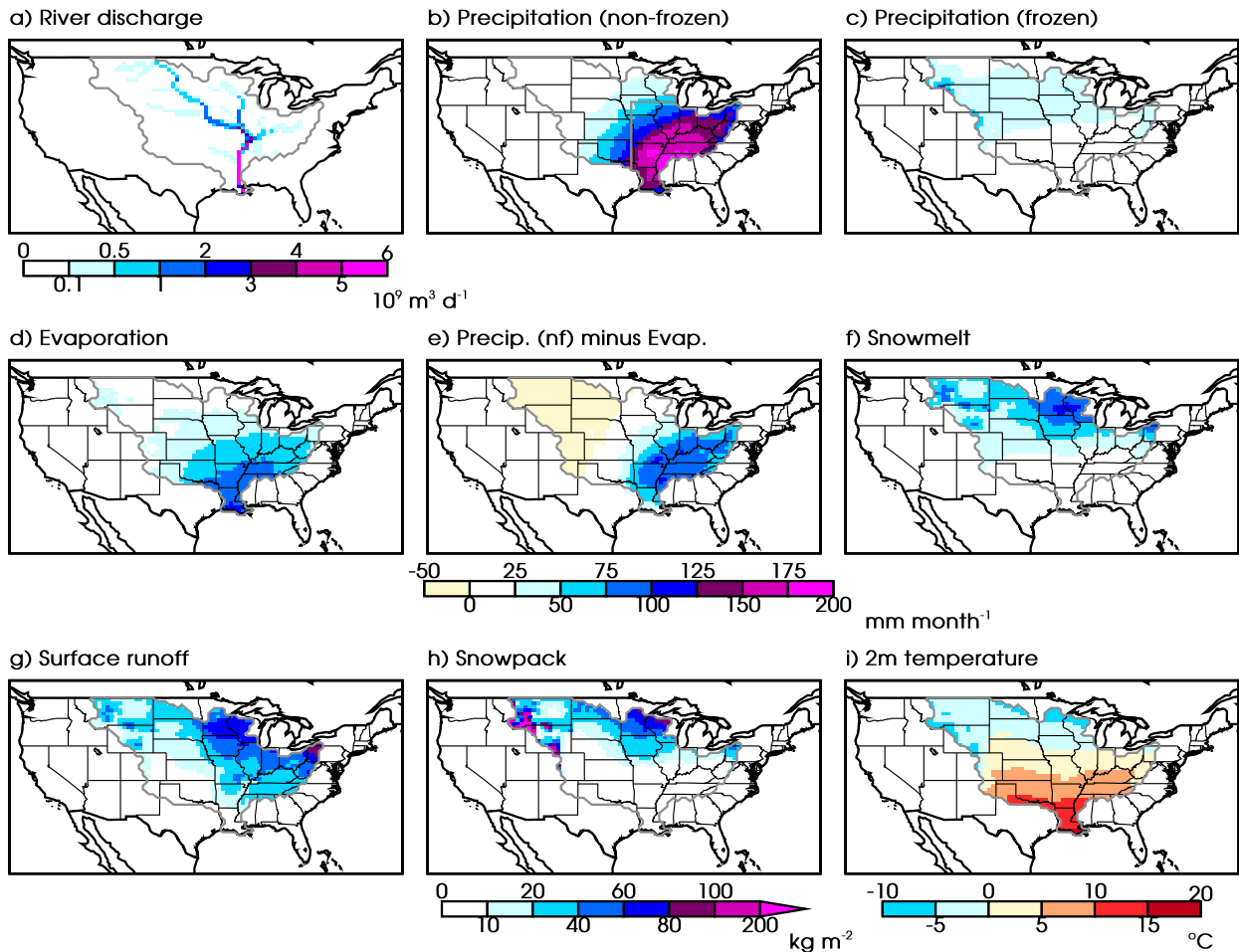


FIG. 5. Composites of the 100-yr high discharge events for (a) river discharge, (b) P_{NF} , (c) frozen precipitation, (d) E , (e) $P_{NF} - E$, (f) SM, (g) R , (h) accumulated snowpack, and (i) 2-m air temperature. Panels (b)–(g) share the same color bar, shown underneath (e).

Missouri (36%), upper Mississippi (25%), and Ohio (22%) catchments, the Arkansas–White–Red, lower Mississippi, and Tennessee contribute much less (7%, 5%, and 5%, respectively). From the available model data, it is not possible to determine what fraction of discharge during events results from $P_{NF} - E$ and what fraction results from snowmelt. However, from the composites we find that the flux of snow meltwater ($4.28 \times 10^9 \text{ m}^3 \text{ day}^{-1}$ in the total basin of Fig. 5f) exceeds that from $P_{NF} - E$ ($2.94 \times 10^9 \text{ m}^3 \text{ day}^{-1}$ in the southeast basin of Fig. 5e). The snowmelt anomalies are greater than the precipitation anomalies (Figs. 6e,f).

Summarizing, we find that, in the GCM, 100-yr high discharge events are related to above-average rainfall in the Ohio and Tennessee catchments and high snowmelt in the northern Missouri, upper Mississippi, and Ohio catchments. Greater snowmelt is a better predictor for extreme river discharge than high precipitation. Note that the analysis is based on a static 1860 modeled

climate. Biases in modeled fields, for example, precipitation, may affect the results, and failure of soil (and surface waters) to store a realistic amount of water may lead to an overestimation of the role of snowmelt in the northwest of the Missouri catchment. Furthermore, climatic changes since 1860 may have changed the relative roles of snowmelt and precipitation in extreme floods; such changes are investigated later in this paper.

5. Predictability of 100-yr extreme discharge events

Next, we investigate cumulative precipitation, the buildup of snowpack, and cumulative snowmelt throughout the winter season. The characteristics associated with extreme high discharge events described in section 4 did not take into account potential time-lagged effects of precipitation and snowmelt leading to these events in FMA. Such effects would enter through the storage term S in Eq. (1). However, winter meteorological conditions are important for spring

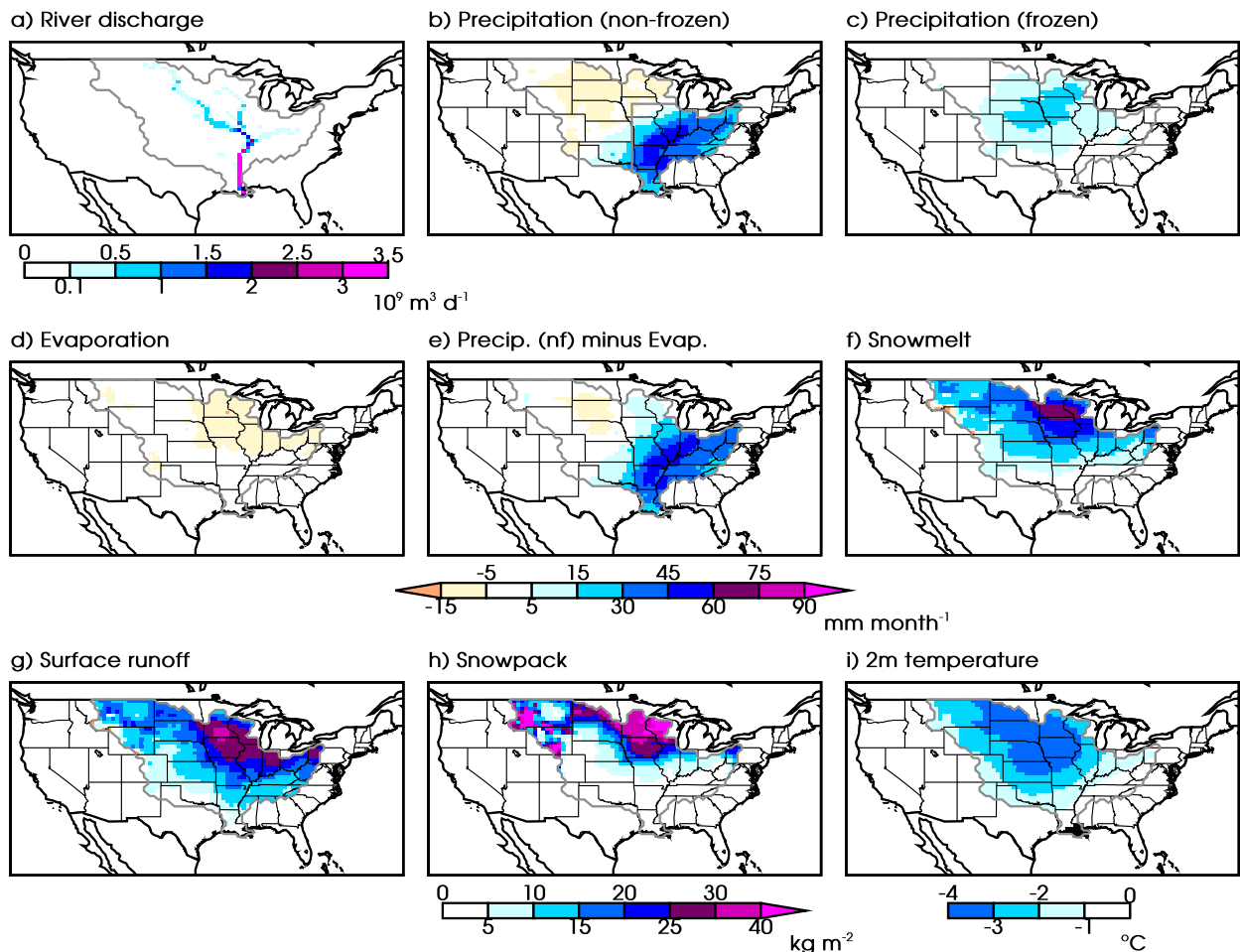


FIG. 6. As in Fig. 5, but for anomalies relative to the mean seasonal cycle of the same variables.

discharge as their effects can accumulate over time in certain land variables and make the land surface more or less susceptible for flooding. This is especially relevant in basins with accumulation of snowpack.

River discharge in the months leading up to the selected 5- and 100-yr high discharge events is above normal in all months considered, though within one standard deviation of interannual variability (Fig. 7a). In March and April, discharge exceeds one standard deviation. This is a direct result of the selection and composite method used here. For the extreme discharge events of interest here (100-yr return time) anomalous high discharge conditions continue into May, beyond the months of selected events (FMA), indicating the long-lasting effects of these events.

Cumulative southeast basin total nonfrozen precipitation (time sum from September preceding the events; Fig. 7b) is above normal in the months leading up to extreme high discharge events, but never exceeds one standard deviation. Time integration was performed as an indicator of effects on subsurface saturation. Similar

analysis of the normal time series gives the same results. Cumulative southeast basin total $P_{NF} - E$ (Fig. 7c) has a comparable progression, though in April and May the values exceed one standard deviation. Following such above-normal wet periods, the river system is likely more susceptible to flooding. Subsurface data, which were not saved for these experiments, would be needed to verify if the land surface is close to or at field capacity.

Cumulative basin total frozen precipitation is above normal and exceeds one standard deviation from January preceding the extreme high discharge events onward (Fig. 7b). The winters preceding selected events are colder than normal, below one standard deviation, in February and March (Fig. 7f). Anomalous frozen precipitation and cold temperatures lead to greater than normal cumulative basin total snowpack (Fig. 7e). Snowpack in the Mississippi catchment builds from October onward and stores water in the catchment for later release into the river system. Climatologically, snowpack peaks in February. In the years of the extreme

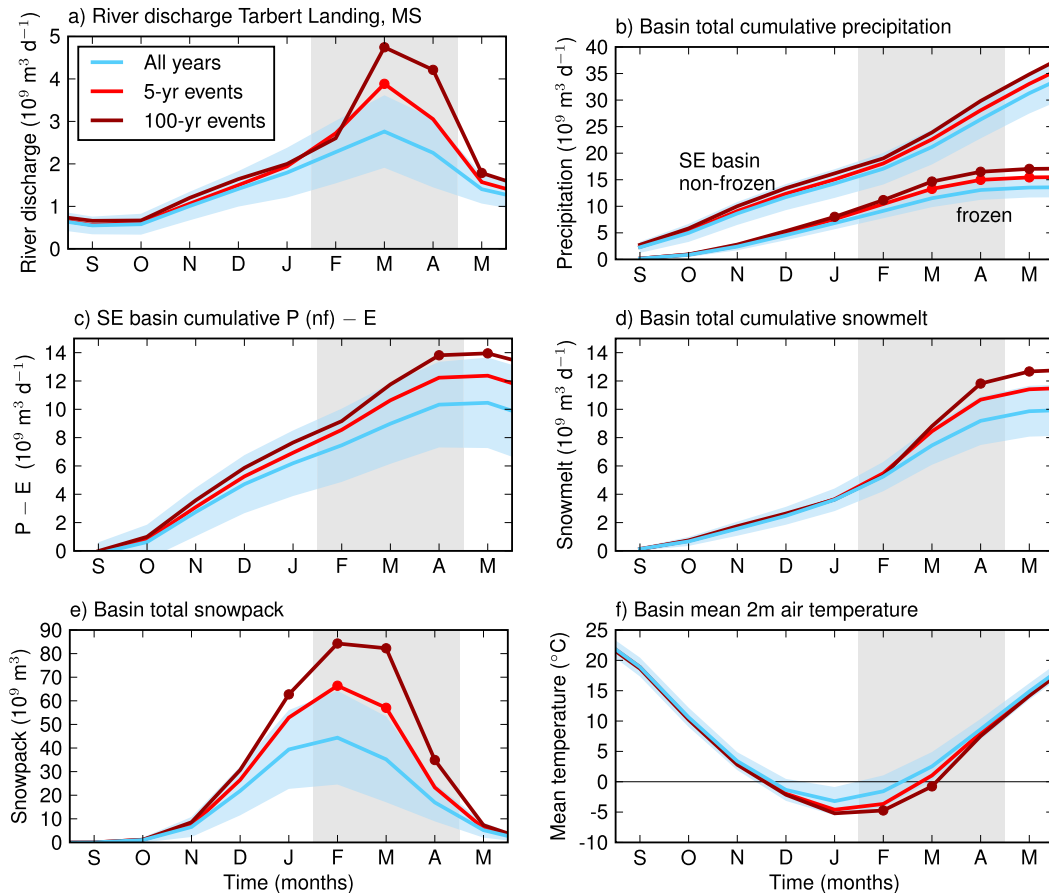


FIG. 7. Climatological time series of different variables in blue lines: (a) river discharge at Tarbert Landing, (b) cumulative southeast basin total P_{NF} and cumulative basin total frozen precipitation, (c) cumulative southeast basin total $P_{NF} - E$, (d) cumulative basin total SM, (e) basin total snowpack, and (f) basin mean 2-m air temperature. Time integration starts from September in the year preceding the selected events. Light blue shading indicates interannual variability (± 1 standard deviation). Overlaid are composite data for the years with 5- and 100-yr return high river discharge events (red and maroon lines, respectively); marker dots indicate when the composite lies outside ± 1 standard deviation. Gray shading shows the months of the composited river discharge events, and left of the gray shading are the months preceding these events.

high discharge events, the maximum buildup snowpack is about double that of the climatological peak (84 and $44 \times 10^9 \text{ m}^3$, respectively). High snowpack in these years fuels anomalous large snowmelt in spring (Fig. 7d).

Anomalous large snowpack may provide some predictability of major Mississippi floods in the months before the event (Maurer and Lettenmaier 2003). We explore a very simple risk analysis scheme, in which seasons with a higher risk of extreme river discharge are selected based on the 10%, 20%, or 30% highest snowpacks from various preceding months (Table 2). To evaluate this scheme, we count the number of extreme discharge events that occur in months after the selected months of the scheme; the maximum would be all events (i.e., 34). Based on this simple scheme, warnings issued in January, based on the top 10% snowpack seasons, would have captured 17 events

(50%). Though these warnings shows some skill (statistically significant at $\alpha = 0.05$), it also means 50% of the events were missed and in 323 years (out of 3400, 9.5% of all years) a false warning is issued. Predicting extreme high discharge events is difficult, due to the many atmospheric and land variables that interact to create such events and the different time scales at which they act. Further complicating our risk analysis, this warning system has been tested on a static 1860 climate in a model, which may not translate to skill in the present day.

6. Future changes of 100-yr extreme discharge events

Finally, we investigate whether the modeled Mississippi risk of extreme high discharge events and drivers

TABLE 2. Number of predicted extreme high discharge events when selecting seasons by extreme high built-up snowpack; percentages of all selected events are in parentheses. Rows indicate the month in which snowpack is considered (preceding the 100-yr events in FMA, for February only discharge events in March and April are considered). Columns indicate the percentage of months considered (i.e., top 10% snowpack for a given month).

	10%	20%	30%
October (FMA)	2 (6%)	10 (29%)	16 (47%)
November	6 (18%)	12 (35%)	16 (47%)
December	8 (24%)	12 (35%)	17 (50%)
January	17 (50%)	25 (74%)	26 (76%)
February (MA)	22 (65%)	27 (79%)	28 (82%)

of such events change in response to global climate change. For this we use the transient forcing model experiment covering 1861–2100 using all five ensemble members and look for trends in the occurrence of extreme events. To do so, the full record is divided into six sections of 40 calendar years each (i.e., there are $5 \times 40 = 200$ years of data in each section). For each section the number of peak-over-threshold events is computed, with the threshold being determined by the level of discharge, precipitation or snowmelt of a given return period based on all years in the experiment (1861–2100).

We find statistically significant negative trends in the occurrence of river discharge events of a 20-, 5-, and 1-yr return period (risk ratio 0.14, 0.14, and 0.33, respectively), but not for discharge events of 100-yr return period (risk ratio 1.0; Fig. 8a). This could have two reasons: either the most extreme Mississippi discharge events are not sensitive to changes in atmospheric greenhouse gas concentrations, ozone, and aerosols, while less extreme events are, or the amount of data in each 40-yr section is insufficient to sample these very rare events leading to a false conclusion. For the less extreme events, the decrease of flood risk practically means that what used to be a 20-yr event in the preindustrial climate will be a 100-yr event at the end of the twenty-first century.

These trends in the occurrence of less extreme discharge events coincide with significant positive trends in extreme precipitation events and significant negative trends in extreme snowmelt events. The probability of extreme precipitation events increases significantly, and the increase is larger for more extreme events (Fig. 8b). For the 100-yr event the increase is so large that the risk ratio is infinite ($p_{1861} = 0$). In practice that means that the extreme events in the future exceed anything that occurred in preindustrial times. The lesser extremes have risk ratios of 64, 5.4, and 2.2 for 20-, 5-, and 1-yr events, respectively. Modeled extreme snowmelt events decrease significantly in response to the prescribed climate change

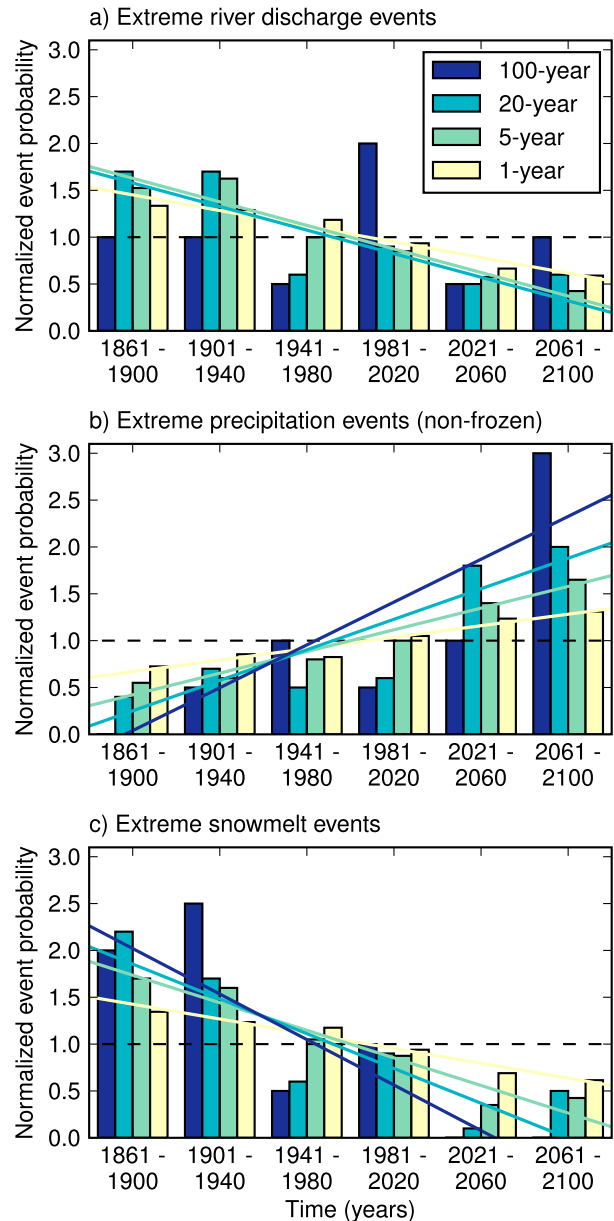


FIG. 8. Normalized probability of extreme (a) river discharge events, (b) southeast catchment-integrated P_{NF} , and (c) catchment-integrated SM in the long transient ensemble experiment (FMA only). Probability is based on a peak-over-threshold approach, with the threshold defined by an event of given return period over the entire integration length. Data from all ensemble members were used. Colored lines show a linear regression of the data, only shown if the slope is significantly different from zero ($\alpha = 0.05$).

forcing (Fig. 8c). As for precipitation events, more extreme events exhibit a larger change than less extreme events. The 100-yr snowmelt event does not occur after 2021, giving a risk ratio of 0 ($p_{2100} = 0$). Less extreme events show a weaker, but still significant, decreasing trend. Risk ratios are between 0 and 0.36.

The annual cycle of these variables is also projected to change. Modeled annual mean nonfrozen precipitation is expected to increase by $0.46 \times 10^9 \text{ m}^3 \text{ day}^{-1}$ (Fig. 9b), in agreement with observed changes in the basin (USGCRP 2017). Part of this increase is a shift from frozen to nonfrozen precipitation in the winter months (annual mean decrease of $0.11 \times 10^9 \text{ m}^3 \text{ day}^{-1}$ in frozen precipitation). The spring snowmelt is much weaker: by -0.49 and $-0.87 \times 10^9 \text{ m}^3 \text{ day}^{-1}$ in March and April, respectively. Likely these changes are a direct result of increased temperatures—the annual mean temperature increase in these simulations is 2.6°C (Fig. 9d; also observed by USGCRP 2017)—and increases in evaporation (figure not shown; southeast basin total evaporation increases by $0.42 \times 10^9 \text{ m}^3 \text{ day}^{-1}$, in agreement with observed increases; Milly and Dunne 2001).

These changes ultimately lead to modeled mean river discharge decreases from November to May, in contrast to observed mean changes (Zhang and Schilling 2006; USGCRP 2017). The largest decrease in the model river occurs during the spring peak, which shifts in the transient experiment from $2.85 \times 10^9 \text{ m}^3 \text{ day}^{-1}$ in 1861–1900 to $2.30 \times 10^9 \text{ m}^3 \text{ day}^{-1}$ in 2061–2100 (Fig. 9a). In the model, the future river is therefore less prone to extreme discharge levels during these months, which may be one reason for the projected decrease in the occurrence of extreme high discharge events.

7. Discussion

Given the negative impact of past floods in the Mississippi catchment and expected future changes in extreme precipitation and snowmelt (Van der Wiel et al. 2016; Kapnick and Hall 2012), we sought to explore characteristics and changes in high discharge events in a fully coupled climate system. We have performed an analysis of 100-yr Mississippi River high discharge events in a fully coupled GCM with an integrated river routing module allowing for an exploration of the interaction between the atmosphere, cryosphere, and land surface in a consistent framework. By means of two experiments, a new model-based hypothesis for the characteristics of these events and the interactions between land and atmosphere in the modeled, physically consistent climate system have been described. In this section we provide a summary of the main results from the model experiments: the characteristics of extreme discharge events and projections for a warmer future based on the GCM. We discuss the validity of these results in the real world given the model limitations and biases, and we provide some suggestions for how these model results may be compared to observational data.

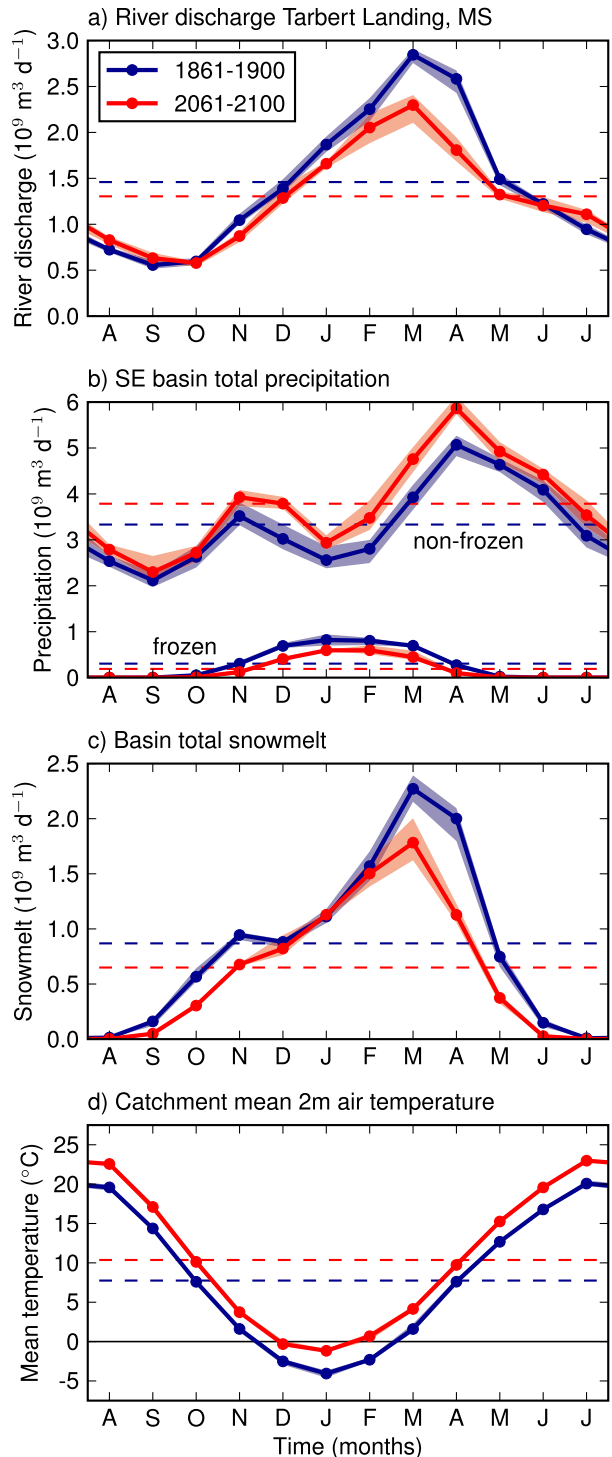


FIG. 9. Change in the annual cycle of (a) river discharge at Tarbert Landing, (b) southeast catchment-integrated nonfrozen and frozen precipitation, (c) catchment-integrated SM, and (d) catchment mean 2-m air temperature ($^\circ\text{C}$). Dashed lines show annual mean values. Shading shows the range of individual ensemble members. Change over two periods 1861–1900 (blue) and 2061–2100 (red) in the transient model experiment.

In the GCM extreme high monthly mean river discharge levels (exceeding the 100-yr return level) coincide with anomalous high snowmelt in the northern part of the basin (Missouri, upper Mississippi, Ohio catchments) and anomalous high precipitation in the southeastern part (Ohio, Tennessee, and lower Mississippi catchments). Extreme snowmelt events more regularly coincide with the extreme high discharge events than extreme precipitation events (section 4). The spring seasons in which these events occur are above-average susceptible to flooding because of conditions in the preceding winter season: 1) long-lasting above normal precipitation, potentially leading to saturation of the subsurface, and 2) anomalously high snowfall leading to greater-than-normal buildup of snowpack. The latter in part relies on temperatures being lower than normal and, crucially, below 0°C. Greater snowpack stores additional water in the basin for later release during the spring melt (section 5). Seasonal risk assessment of major events is complicated due to the many variables involved and interactions between them, though a simple scheme based on winter snowpack shows some skill.

In the GCM, human-induced climate change does not lead to a statistically significant trend in the occurrences of 100-yr extreme high discharge events, though smaller events of 20-, 5-, and 1-yr return periods are projected to occur less frequently in a warmer climate (section 6). Empirically, Hodgkins et al. (2017) show that major and minor floods may exhibit different trends. Physical explanations for the different responses to increasing atmospheric greenhouse gas concentrations may be found in different forcing mechanisms for major and minor floods (section 4).

The modeled decrease of high discharge events may be caused by decreasing snowmelt. The GCM projects a shift from frozen to nonfrozen precipitation, a weaker climatological spring melt, and fewer extreme snowmelt events. Snowmelt depends on the accumulation of snowpack; the spring melt is therefore very sensitive to changing wintertime temperatures. Extreme precipitation events are projected to increase with climate change, and this would have an opposing effect on high discharge events. The contrasting trends of snowmelt and precipitation may lead to a change in the characteristics of extreme discharge events and may be responsible for the absence of a trend in discharge events. Though, despite long experimental integrations, sampling size remains an issue for the 100-yr events and may impact the modeled trend. Further experiments with the GCM are needed to investigate the potential change in forcing mechanisms in more detail. Regime shifts away from snowmelt-dominated rivers have been reported previously for other basins (e.g., Nijssen et al. 2001; Barnett et al. 2005; Immerzeel et al. 2010).

The presented results crucially depend on the assumption that the FLOR GCM adequately captures the relationship between meteorological conditions, land processes, and river discharge. As noted in section 3, simulated discharge is biased toward an early spring peak (Figs. 1c,d). This bias is affected by numerous processes that are not easily constrained in the model: spring convective rain events may be too strong; regional snowmelt could occur early; infiltration could be excessively suppressed on frozen ground, effectively removing subsurface storage delay; and possibly storage in the surface waters could be biased low. In the model, the spring discharge bias coincides with a positive precipitation bias and lower-than-observed snowpack (Figs. 1e,f). Both these biases likely contribute to the discharge bias; excessive precipitation directly contributes to extra river water, and low snowpack values lead to a more rapid snowmelt during warmer months due to the thermal inertia of snowpack and surface albedo feedbacks (Hall and Qu 2006; Kapnick and Hall 2012). Snowmelt in far northwest Missouri coinciding with precipitation in the Tennessee area is unlikely to contribute to the same flood in the real world. In the observed record, lower Mississippi floods have often been directly linked to sequences of severe convective storms (e.g., Smith and Baeck 2015). To assess the impacts of model biases on the results, we suggest performing a similar analysis with future versions of the model with various adjustments made to less-constrained hydrologic parameters. To investigate the model sensitivity of the results, a repetition using different GCMs is required, though careful consideration of the ability of the models to capture the required processes is needed.

The difference between the reported characteristics of extreme discharge events in the model and those for observed flood events may also be caused by a mismatch of instantaneous discharge extremes and monthly mean extremes (Fig. 2). Likely, instantaneous discharge peaks are more closely related to extreme precipitation events in the lower Ohio, lower Arkansas, and Tennessee catchments than monthly mean peaks are. A future study based on daily data is required to quantify the impact of the chosen monthly basis of the presented results. Such an analysis would allow for a study of the sequence of weather events leading up to major discharge events.

Trends in observed extreme river discharge events are difficult to identify because discharge changes due to climate change may be obscured by discharge changes caused by changes in land use, irrigation practices, or river management (Potter 1991; Zhang and Schilling 2006; Mao and Cherkauer 2009; Munoz et al. 2018). Further complicating such analysis is the limited length of data that is often available, providing only small

sample sizes (Fig. 3) and potentially masking decadal variations. Reported trends of discharge in (tributaries of) the Mississippi are small and sometimes inconsistent with meteorological changes (e.g., Lettenmaier et al. 1994; Lins and Slack 1999; Olsen et al. 1999; Rossi et al. 2009). Previous modeling studies are in agreement with this study and report a slight decrease in flood risk of the Mississippi (e.g., Nijssen et al. 2001; Milly et al. 2002; Arnell 2003; Aerts et al. 2006; Hirabayashi et al. 2013; Van Vliet et al. 2013), though Arnell and Gosling (2016) show flood risk projections are sensitive to climate model choice.

The presented results are based on a physically consistent climate, but feedbacks and sensitivities in the modeled climate may differ from those in the natural environment. Future work should therefore focus on testing the presented results using observational data and experiences during historic floodings. We note, however, that extensive time series of snowpack and snowmelt data do not exist, and therefore, the role of snowmelt, or other land processes, in river flooding cannot be investigated in much detail. Our perception of floods may consequently be susceptible for biases toward precipitation-forced flooding events, given that analysis of precipitation–river discharge relationships is possible with observed data (e.g., Smith and Baeck 2015; Berghuijs et al. 2016; Benedict et al. 2018). Efforts should be placed in improving our future ability to further constrain snowpack in GCMs; this can be achieved with enhanced and sustained snowpack measurements. This is crucial for improving our understanding of the full extent of the climate sensitivity of the regional hydrology, including Mississippi River discharge, to snowpack loss in a warming climate. Furthermore, short observed time series or model experiments allow for investigation of weaker extreme events only. Extrapolation of mechanisms and trends to apply to major extreme events needs to be done with care and with consideration that forcing mechanisms may differ, as was shown to be the case in the model.

For adequate flood risk management, understanding extreme flood characteristics is vital. Because buildings and infrastructure projects are built to be used in later decades, consideration of the effects of anthropogenic climate change is necessary. Other human processes impacting extreme river discharge, most notably river management by means of dams, reservoirs, and canals, were not considered in the current study. Including current and future impacts of human processes in a similar study would therefore provide valuable insights.

Despite its limitations, the novel impact-based modeling approach applied in this study provides a framework for analysis of meteorological and land drivers of

extreme societal impact events. Because FLOR GCM models the coupled atmosphere–land–river system, the presented flooding hypothesis is physically consistent and its water budget is closed by definition. Given the continuously increasing complexity of GCMs, more societally relevant variables can be readily modeled. Therefore, in the future, an increasing number of climate-induced impact events may be investigated following a similar approach.

Acknowledgments. We thank Nathaniel Chaney, Tom Delworth, and two anonymous reviewers for their comments, which helped to improve the manuscript. This report was prepared by Karin van der Wiel under Award NA14OAR4320106 from the National Oceanic and Atmospheric Administration, U.S. Department of Commerce. The statements, findings, conclusions, and recommendations are those of the author(s) and do not necessarily reflect the views of the National Oceanic and Atmospheric Administration, or the U.S. Department of Commerce. The data reported in this paper have been deposited in the Geophysical Fluid Dynamics Laboratory Data Portal (available at data1.gfdl.noaa.gov/).

REFERENCES

- Aerts, J., H. Renssen, P. Ward, H. de Moel, E. Odada, L. Bouwer, and H. Goosse, 2006: Sensitivity of global river discharges under Holocene and future climate conditions. *Geophys. Res. Lett.*, **33**, L19401, <https://doi.org/10.1029/2006GL027493>.
- Arnell, N. W., 2003: Effects of IPCC SRES* emissions scenarios on river runoff: A global perspective. *Hydrol. Earth Syst. Sci.*, **7**, 619–641, <https://doi.org/10.5194/hess-7-619-2003>.
- , and S. N. Gosling, 2016: The impacts of climate change on river flood risk at the global scale. *Climatic Change*, **134**, 387–401, <https://doi.org/10.1007/s10584-014-1084-5>.
- Barnett, T. P., J. C. Adam, and D. P. Lettenmaier, 2005: Potential impacts of a warming climate on water availability in snow-dominated regions. *Nature*, **438**, 303–309, <https://doi.org/10.1038/nature04141>.
- Bayard, D., M. Stähli, A. Parriaux, and H. Flüeler, 2005: The influence of seasonally frozen soil on the snowmelt runoff at two Alpine sites in southern Switzerland. *J. Hydrol.*, **309**, 66–84, <https://doi.org/10.1016/j.jhydrol.2004.11.012>.
- Benedict, I., C. C. van Heerwaarden, A. H. Weerts, and W. Hazeleger, 2018: An evaluation of the importance of spatial resolution in a global climate and hydrological models based on the Rhine and Mississippi basins. *Hydrol. Earth Syst. Sci. Discuss.*, <https://doi.org/10.5194/hess-2018-437>.
- Berghuijs, W. R., R. A. Woods, C. J. Hutton, and M. Sivapalan, 2016: Dominant flood generating mechanisms across the United States. *Geophys. Res. Lett.*, **43**, 4382–4390, <https://doi.org/10.1002/2016GL068070>.
- Camillo, C. A., 2012: *Divine Providence: The 2011 Flood in the Mississippi River and Tributaries Project*. Mississippi River Commission, 328 pp.
- Changnon, S. A., 1998: The historical struggle with floods on the Mississippi River basin: Impacts of recent floods and lessons

- for future flood management and policy. *Water Int.*, **23**, 263–271, <https://doi.org/10.1080/02508069808686781>.
- Cherkauer, K. A., and D. P. Lettenmaier, 1999: Hydrologic effects of frozen soils in the upper Mississippi River basin. *J. Geophys. Res.*, **104**, 19 599–19 610, <https://doi.org/10.1029/1999JD900337>.
- Delworth, T. L., and Coauthors, 2006: GFDL's CM2 global coupled climate models. Part I: Formulation and simulation characteristics. *J. Climate*, **19**, 643–674, <https://doi.org/10.1175/JCLI3629.1>.
- , and Coauthors, 2012: Simulated climate and climate change in the GFDL CM2.5 high-resolution coupled climate model. *J. Climate*, **25**, 2755–2781, <https://doi.org/10.1175/JCLI-D-11-00316.1>.
- De Michele, C., and G. Salvadori, 2002: On the derived flood frequency distribution: Analytical formulation and the influence of antecedent soil moisture condition. *J. Hydrol.*, **262**, 245–258, [https://doi.org/10.1016/S0022-1694\(02\)00025-2](https://doi.org/10.1016/S0022-1694(02)00025-2).
- Donner, S. D., and D. Scavia, 2007: How climate controls the flux of nitrogen by the Mississippi River and the development of hypoxia in the Gulf of Mexico. *Limnol. Oceanogr.*, **52**, 856–861, <https://doi.org/10.4319/lo.2007.52.2.0856>.
- FEMA, 2017: National flood insurance program: Flood hazard mapping. Accessed 5 September 2018, <https://www.fema.gov/national-flood-insurance-program-flood-hazard-mapping>.
- Foley, J. A., C. J. Kucharik, T. E. Twine, M. T. Coe, and S. D. Donner, 2004: Land use, land cover, and climate change across the Mississippi basin: Impacts on selected land and water resources. *Ecosystems and Land Use Change*, *Geophys. Monogr.*, Vol. 153, Amer. Geophys. Union, 249–261, <https://doi.org/10.1029/153GM19>.
- Galloway, G. E., Jr., 1995: Learning from the Mississippi flood of 1993: Impacts, management issues, and areas for research. *Proc. U.S.–Italy Workshop on the Hydrometeorology, Impacts, and Management of Extreme Floods*, Perugia, Italy, Colorado State University/University of Genova, 29 pp., <https://www.engr.colostate.edu/ce/facultystaff/salas/us-italy/papers/12galloway.pdf>.
- George, S. S., 2018: Mississippi rising. *Nature*, **556**, 34–35, <https://doi.org/10.1038/d41586-018-03243-z>.
- Hall, A., and X. Qu, 2006: Using the current seasonal cycle to constrain snow albedo feedback in future climate change. *Geophys. Res. Lett.*, **33**, L03502, <https://doi.org/10.1029/2005GL025127>.
- Harmar, O. P., N. J. Clifford, C. R. Thorne, and D. S. Biedenharn, 2005: Morphological changes of the lower Mississippi river: Geomorphological response to engineering intervention. *River Res. Appl.*, **21**, 1107–1131, <https://doi.org/10.1002/rra.887>.
- Higgins, R. W., W. Shi, E. Yarosh, and R. Joyce, 2000: Improved United States precipitation quality control system and analysis. NCEP/Climate Prediction Center ATLAS 7, http://www.cpc.ncep.noaa.gov/research_papers/ncep_cpc_atlas/7/toc.html.
- Hirabayashi, Y., R. Mahendran, S. Koirala, L. Konoshima, D. Yamazaki, S. Watanabe, H. Kim, and S. Kanae, 2013: Global flood risk under climate change. *Nat. Climate Change*, **3**, 816–821, <https://doi.org/10.1038/nclimate1911>.
- Hodgkins, G. A., and Coauthors, 2017: Climate-driven variability in the occurrence of major floods across North America and Europe. *J. Hydrol.*, **552**, 704–717, <https://doi.org/10.1016/j.jhydrol.2017.07.027>.
- Immerzeel, W. W., L. P. Van Beek, and M. F. Bierkens, 2010: Climate change will affect the Asian water towers. *Science*, **328**, 1382–1385, <https://doi.org/10.1126/science.1183188>.
- Jia, L., and Coauthors, 2015: Improved seasonal prediction of temperature and precipitation over land in a high-resolution GFDL climate model. *J. Climate*, **28**, 2044–2062, <https://doi.org/10.1175/JCLI-D-14-00112.1>.
- , and Coauthors, 2016: The roles of radiative forcing, sea surface temperatures, and atmospheric and land initial conditions in U.S. summer warming episodes. *J. Climate*, **29**, 4121–4135, <https://doi.org/10.1175/JCLI-D-15-0471.1>.
- Kapnick, S. B., and A. Hall, 2012: Causes of recent changes in western North American snowpack. *Climate Dyn.*, **38**, 1885–1899, <https://doi.org/10.1007/s00382-011-1089-y>.
- , and T. L. Delworth, 2013: Controls of global snow under a changed climate. *J. Climate*, **26**, 5537–5562, <https://doi.org/10.1175/JCLI-D-12-00528.1>.
- Krishnamurthy, L., and Coauthors, 2018: Causes and probability of occurrence of extreme precipitation events like Chennai 2015. *J. Climate*, **31**, 3831–3848, <https://doi.org/10.1175/JCLI-D-17-0302.1>.
- Kunkel, K. E., R. A. Pielke Jr., and S. A. Changnon, 1999: Temporal fluctuations in weather and climate extremes that cause economic and human health impacts: A review. *Bull. Amer. Meteor. Soc.*, **80**, 1077, [https://doi.org/10.1175/1520-0477\(1999\)080<1077:TFIWAC>2.0.CO;2](https://doi.org/10.1175/1520-0477(1999)080<1077:TFIWAC>2.0.CO;2).
- Lettenmaier, D. P., E. F. Wood, and J. R. Wallis, 1994: Hydroclimatological trends in the continental United States, 1948–88. *J. Climate*, **7**, 586–607, [https://doi.org/10.1175/1520-0442\(1994\)007<0586:HCTITC>2.0.CO;2](https://doi.org/10.1175/1520-0442(1994)007<0586:HCTITC>2.0.CO;2).
- Lins, H. F., and J. R. Slack, 1999: Streamflow trends in the United States. *Geophys. Res. Lett.*, **26**, 227–230, <https://doi.org/10.1029/1998GL900291>.
- Lott, G. A., and V. A. Myers, 1956: Meteorology of flood-producing storms in the Mississippi River basin. Weather Bureau Hydrometeorological Rep. 34, 226 pp.
- Mao, D., and K. A. Cherkauer, 2009: Impacts of land-use change on hydrologic responses in the Great Lakes region. *J. Hydrol.*, **374**, 71–82, <https://doi.org/10.1016/j.jhydrol.2009.06.016>.
- Maurer, E. P., and D. P. Lettenmaier, 2003: Predictability of seasonal runoff in the Mississippi river basin. *J. Geophys. Res.*, **108**, 8607, <https://doi.org/10.1029/2002JD002555>.
- Merz, R., and G. Blöschl, 2003: Regional flood risk—What are the driving processes? *IAHS Publ.*, **281**, 49–58, http://hydrologie.org/redbooks/a281/iahs_281_049.pdf.
- Milly, P. C. D., and K. Dunne, 2001: Trends in evaporation and surface cooling in the Mississippi river basin. *Geophys. Res. Lett.*, **28**, 1219–1222, <https://doi.org/10.1029/2000GL012321>.
- , and K. A. Dunne, 2017: A hydrologic drying bias in water-resource impact analyses of anthropogenic climate change. *J. Amer. Water Resour. Assoc.*, **53**, 822–838, <https://doi.org/10.1111/1752-1688.12538>.
- , R. T. Wetherald, K. Dunne, and T. L. Delworth, 2002: Increasing risk of great floods in a changing climate. *Nature*, **415**, 514–517, <https://doi.org/10.1038/415514a>.
- , and Coauthors, 2014: An enhanced model of land water and energy for global hydrologic and earth-system studies. *J. Hydrometeorol.*, **15**, 1739–1761, <https://doi.org/10.1175/JHM-D-13-0162.1>.
- Munoz, S. E., and Coauthors, 2018: Climatic control of Mississippi river flood hazard amplified by river engineering. *Nature*, **556**, 95–98, <https://doi.org/10.1038/nature26145>.
- Murakami, H., and Coauthors, 2017: Dominant role of subtropical Pacific warming in extreme eastern Pacific hurricane seasons: 2015 and the future. *J. Climate*, **30**, 243–264, <https://doi.org/10.1175/JCLI-D-16-0424.1>.
- Myers, V. A., 1959: Meteorology of hypothetical flood sequences in the Mississippi River basin. Weather Bureau Hydrometeorological Rep. 35, 45 pp.

- National Operational Hydrologic Remote Sensing Center, 2004: Snow data assimilation system (SNODAS) data products at NSIDC, version 1. National Snow and Ice Data Center, accessed 20 April 2018, <https://doi.org/10.7265/N5TB14TC>.
- Nijssen, B., G. M. O'Donnell, A. F. Hamlet, and D. P. Lettenmaier, 2001: Hydrologic sensitivity of global rivers to climate change. *Climatic Change*, **50**, 143–175, <https://doi.org/10.1023/A:1010616428763>.
- O'Gorman, P. A., 2015: Precipitation extremes under climate change. *Curr. Clim. Change Rep.*, **1**, 49–59, <https://doi.org/10.1007/s40641-015-0009-3>.
- Olsen, J. R., J. R. Stedinger, N. C. Matalas, and E. Z. Stakhiv, 1999: Climate variability and flood frequency estimation for the upper Mississippi and lower Missouri Rivers. *J. Amer. Water Resour. Assoc.*, **35**, 1509–1523, <https://doi.org/10.1111/j.1752-1688.1999.tb04234.x>.
- Pinter, N., R. R. van der Ploeg, P. Schweigert, and G. Hoefler, 2006: Flood magnification on the River Rhine. *Hydrol. Processes*, **20**, 147–164, <https://doi.org/10.1002/hyp.5908>.
- , A. A. Jemberie, J. W. Remo, R. A. Heine, and B. S. Ickes, 2010: Cumulative impacts of river engineering, Mississippi and Lower Missouri rivers. *River Res. Appl.*, **26**, 546–571, <https://doi.org/10.1002/rra.1269>.
- Potter, K. W., 1991: Hydrological impacts of changing land management practices in a moderate-sized agricultural catchment. *Water Resour. Res.*, **27**, 845–855, <https://doi.org/10.1029/91WR00076>.
- Rabalais, N. N., R. E. Turner, W. J. Wiseman Jr., and Q. Dortch, 1998: Consequences of the 1993 Mississippi River flood in the Gulf of Mexico. *River Res. Appl.*, **14**, 161–177, [https://doi.org/10.1002/\(SICI\)1099-1646\(199803/04\)14:2<161::AID-RRR495>3.0.CO;2-J](https://doi.org/10.1002/(SICI)1099-1646(199803/04)14:2<161::AID-RRR495>3.0.CO;2-J).
- Raymond, P. A., N.-H. Oh, R. E. Turner, and W. Broussard, 2008: Anthropogenically enhanced fluxes of water and carbon from the Mississippi river. *Nature*, **451**, 449, <https://doi.org/10.1038/nature06505>.
- Rossi, A., N. Massei, B. Laignel, D. Sebag, and Y. Copard, 2009: The response of the Mississippi River to climate fluctuations and reservoir construction as indicated by wavelet analysis of streamflow and suspended-sediment load, 1950–1975. *J. Hydrol.*, **377**, 237–244, <https://doi.org/10.1016/j.jhydrol.2009.08.032>.
- Shevliakova, E., and Coauthors, 2009: Carbon cycling under 300 years of land use change: Importance of the secondary vegetation sink. *Global Biogeochem. Cycles*, **23**, GB2022, <https://doi.org/10.1029/2007GB003176>.
- Smith, J. A., and M. L. Baeck, 2015: “Prophetic vision, vivid imagination”: The 1927 Mississippi River flood. *Water Resour. Res.*, **51**, 9964–9994, <https://doi.org/10.1002/2015WR017927>.
- Tramblay, Y., C. Bouvier, C. Martin, J.-F. Didon-Lescot, D. Todorovik, and J.-M. Domergue, 2010: Assessment of initial soil moisture conditions for event-based rainfall-runoff modelling. *J. Hydrol.*, **387**, 176–187, <https://doi.org/10.1016/j.jhydrol.2010.04.006>.
- USGCRP, 2017: Climate Science Special Report: Fourth National Climate Assessment, Volume 1. D. J. Wuebbles et al., Eds., U.S. Global Change Research Program, 470 pp., <https://doi.org/10.7930/J0J964J6>.
- Van der Wiel, K., and Coauthors, 2016: The resolution dependence of contiguous U.S. precipitation extremes in response to CO₂ forcing. *J. Climate*, **29**, 7991–8012, <https://doi.org/10.1175/JCLI-D-16-0307.1>.
- , and Coauthors, 2017: Rapid attribution of the August 2016 flood-inducing extreme precipitation in south Louisiana to climate change. *Hydrol. Earth Syst. Sci.*, **21**, 897–921, <https://doi.org/10.5194/hess-21-897-2017>.
- Van Vliet, M. T., W. H. Franssen, J. R. Yearsley, F. Ludwig, I. Haddeland, D. P. Lettenmaier, and P. Kabat, 2013: Global river discharge and water temperature under climate change. *Global Environ. Change*, **23**, 450–464, <https://doi.org/10.1016/j.gloenvcha.2012.11.002>.
- Van Vuuren, D. P., and Coauthors, 2011: The representative concentration pathways: An overview. *Climatic Change*, **109**, 5–31, <https://doi.org/10.1007/s10584-011-0148-z>.
- Vecchi, G. A., and Coauthors, 2014: On the seasonal forecasting of regional tropical cyclone activity. *J. Climate*, **27**, 7994–8016, <https://doi.org/10.1175/JCLI-D-14-00158.1>.
- Wallenfeldt, J., R. A. Muller, G. T. Severin, R. H. Kesel, and R. J. Schaetzl, 2015: Mississippi River. *Encyclopaedia Britannica*, accessed 11 November 2016, <https://www.britannica.com/place/Mississippi-River>.
- Zhang, Y.-K., and K. Schilling, 2006: Increasing streamflow and baseflow in Mississippi River since the 1940s: Effect of land use change. *J. Hydrol.*, **324**, 412–422, <https://doi.org/10.1016/j.jhydrol.2005.09.033>.